Journal of Cerebral Blood Flow & Metabolism (2014) 34, 1810–1817

www.jcbfm.com

ORIGINAL ARTICLE

Metabolic T_1 dynamics and longitudinal relaxation enhancement *in vivo* at ultrahigh magnetic fields on ischemia

Noam Shemesh[1], Jens T Rosenberg[2,3], Jean-Nicolas Dumez[1], Samuel C Grant[2,3] and Lucio Frydman[1,2]

Interruptions in cerebral blood flow may lead to devastating neural outcomes. Magnetic resonance has a central role in diagnosing and monitoring these insufficiencies, as well as in understanding their underlying metabolic consequences. Magnetic resonance spectroscopy (MRS) in particular can probe ischemia via the signatures of endogenous metabolites including lactic acid (Lac), *N*-acetylaspartate, creatine (Cre), and cholines. Typically, MRS reports on these metabolites' concentrations. This study focuses on establishing the potential occurrence of *in vivo* longitudinal relaxation enhancement (LRE) effects—a phenomenon involving a reduction of the apparent T_1 with selective bandwidth excitations— in a rat stroke model at 21.1 T. Statistically significant reductions in Cre's apparent T_1s were observed at all the examined post-ischemia time points for both ipsi- and contralateral hemispheres, thereby establishing the existence of LREs for this metabolite *in vivo*. Ischemia-dependent LRE trends were also noted for Lac in the ipsilateral hemisphere only 24 hours after ischemia. Metabolic T_1s were also found to vary significantly as a function of post-stroke recovery time, with the most remarkable and rapid changes observed for Lac T_1s. The potential of such measurements to understand stroke at a molecular level and assist in its diagnosis, is discussed.

Journal of Cerebral Blood Flow & Metabolism (2014) **34,** 1810–1817; doi:10.1038/jcbfm.2014.149; published online 10 September 2014

Keywords: ischemic stroke; longitudinal relaxation enhancement; magnetic resonance spectroscopy; metabolite–tissue interactions; T_1 relaxation; ultrahigh field MRS

INTRODUCTION

The highly complex functions of the brain depend on an intricate coupling between neural activity, metabolism, and the continuous blood supply needed to meet energetic demands.[1] When cerebral blood flow is interrupted, an 'ischemic cascade' is triggered[1,2] whereby faltering energy supplies alter cellular bioenergetics and shift ion populations between extra- and intracellular spaces. This, in turn, induces excitotoxicity, promoting further tissue injuries. As a result, structural changes to the cellular microstructure will follow, with swelling occurring owing to the osmotic modulations, and ultimately cell death ensues.[3] The overall consequence is a potentially detrimental functional impairment, with often devastating neurologic outcomes.[1–3] Magnetic resonance imaging (MRI) plays a central role in characterizing these central nervous system (CNS) events in general, while providing an early diagnosis of ischemia in particular.[4–6] Most notably, diffusion- and perfusion-weighted MRI of water can be used for identifying the onset of stroke, and help define the treatment-oriented windows of opportunity. Magnetic resonance imaging can further assist in detecting the potentially salvageable penumbra region, and provide quantifiable information about the structural and functional alterations occurring after ischemia.[4–8] Functional MRI can be used to characterize the outcome of a stroke, as well as to follow neural network reorganizations compensating for stroke-induced functional impairments.[9,10]

Magnetic resonance spectroscopy (MRS) is an alternative approach that, although closely related to MRI, focuses on resolving the localized spectral metabolic signatures imparted by endogenous CNS metabolites rather than reflecting the spatial distribution of water.[11] Numerous small molecules can be routinely observed by ^{1}H MRS including bioenergetics-related metabolites (creatines (Cre), lactic acid (Lac)), osmolytes (*N*-acetylaspartate, (NAA)), metabolites participating in membrane synthesis (cholines, (Cho)), and neurotransmitters (glutamate, γ-aminobutyric acid).[11,12] Owing to their participation in underlying metabolism and more selective compartmentation, the relative concentrations of these metabolites—as conventionally quantified from the peak intensities and line shapes—are often sought by MRS scans seeking to evaluate stroke. For example, NAA is considered a neuronal viability biomarker,[13] whereas both Lac and NAA levels correlate with stroke severity and functional outcome.[14] ^{1}H MRS also can be combined with water-based diffusion MRI to improve the clinical prediction of a stroke's repercussions;[15] diffusion[16,17] and ^{1}H MRS studies based on spin–spin (T_2) and spin–lattice (T_1) relaxation times have been proposed as useful complements to reveal more elaborate interactions of metabolites within the host tissues.[18–24]

Another potential source of insight regarding the interaction between metabolites and their host tissues, could arise from investigating longitudinal relaxation enhancement (LRE) effects. Longitudinal relaxation enhancement is a phenomenon exploited

[1]Department of Chemical Physics, Weizmann Institute of Science, Rehovot, Israel; [2]National High Magnetic Field Laboratory, The Florida State University, Tallahassee, Florida, USA and [3]Chemical & Biomedical Engineering, The Florida State University, Tallahassee, Florida, USA. Correspondence: Professor SC Grant, Department of Chemical & Biomedical Engineering, Florida State University, Tallahassee, FL 32310, USA or Professor L Frydman, Department of Chemical Physics, Weizmann Institute of Science, Rehovot 76100, Israel. E-mail: grant@magnet.fsu.edu or lucio.frydman@weizmann.ac.il

This work was supported by the US NSF via the National High Magnetic Field Laboratory (DMR-0654118), the NHMFL User Collaboration Grant Program (awarded to SCG) and its Visiting Scientist Program #12601 (to NS). Additional funding provided by the Israel Science Foundation (Grant ISF 1142/13), the EC Marie Curie Action ITN METAFLUX (project 264780) and the American Heart Association Grant-in-Aid (10GRNT3860040).

Received 7 April 2014; revised 25 July 2014; accepted 28 July 2014; published online 10 September 2014

in biomolecular NMR, for examining amide groups and enhancing signal-to-noise ratios per unit time.[25,26] Longitudinal relaxation enhancement involves a reduction in a resonance's apparent T_1 on switching from a broadband excitation with active water suppression to a spectrally selective excitation targeting only the resonances of interest. By leaving the main solvent reservoir as well as many of the macromolecular protons magnetically unperturbed, a T_1 shortening can be mediated both by chemical exchange phenomena with water, as well as via cross-relaxation effects between the targeted and unperturbed proton reservoirs. Although small molecules (such as brain metabolites) do not generally exhibit LRE effects when dissolved in solutions,[26] we recently found that on executing spectrally selective excitations in *ex vivo* brains, the non-labile methyl resonances of Lac, Cre, and Cho—as well as numerous other labile ^{1}H sites—exhibited significant LREs at 9.4T.[27] These first observations of LRE probably reflect a dynamic binding of these metabolites to macromolecules, facilitating effective cross-relaxation with bound macromolecular protons, or water-related exchange effects in proximate sites of the targeted metabolite. Previous studies also noted a magnetic coupling between the water and Cre methyl resonances *in vivo,*[28,29] as well as magnetization transfer effects between water and Lac's methyl resonance.[30] LREs, as quantified from differences in apparent T_1s on changing from a broadband, water-suppressed excitation to a selective excitation that does not affect the water magnetization, could thus potentially serve as a new type of metabolic reporter.

To validate such premise, the present study aims to (i) determine whether LRE effects previously observed *ex vivo*[27] also affect metabolic resonances *in vivo;* and (ii) examine whether, given the putative influence that binding processes have on these effects, LREs are affected by pathologic processes in brain tissues. To achieve such aims, this study harnesses the high quality ^{1}H MRS spectra that can be obtained under optimized ultrahigh field conditions, and investigates the time dependencies that both metabolic T_1s and LREs exhibit after ischemia. Localized LRE MRS sequences addressing solely the methyl resonances of Lac, Cre, Cho, and NAA were thus implemented, and ^{1}H T_1 behaviors in the presence and absence of water suppression were compared in a rat model subject to a transient occlusion of the middle cerebral artery (MCA). The evolution of these parameters was followed between 3 hours and 1 week after ischemia, using the sensitivity and resolution advantages afforded by the 21.1 T preclinical MRI situated at the US National High Magnetic Field Laboratory. This unique magnet permitted the *in vivo* detection of unequivocal LRE effects for Cre, as well as substantial changes in other metabolic T_1s after ischemia and as a function of stroke recovery. The biophysical origin of these changes and their potential as novel disease biomarkers are discussed.

MATERIALS AND METHODS

All experiments were approved by the Florida State University Animal Care and Use Committee (ACUC protocol #1038). The FSU Animal Research Program has been accredited by the Association for Assessment and Accreditation of Laboratory Animal Care (AAALAC), International. Florida State University is registered as a research facility with the United States Department of Agriculture (Registration #58-R-0001) and has an Animal Welfare Assurance number (#A3854-01) on file with the US Public Health Service. Under the direction of a veterinarian who is certified as a specialist in laboratory animal medicine by the American College of Laboratory Animal Medicine, all animal procedures were undertaken according to these regulatory bodies and AAALAC guidelines, and every effort was taken to minimize animal suffering.

Middle Cerebral Artery Occlusion

All surgical procedures in this study were performed under aseptic conditions. The MCAs of Juvenile Sprague–Dawley rats were occluded for 1.5 hours. Briefly, anesthesia was induced using 5% isoflurane in 100% medical grade O_2 and further maintained with 2% isoflurane. A filament (Doccol Corp., Sharon, MA, USA) was guided 1.9 cm through the external carotid artery, whereupon it blocked blood flow proximal to the MCA. The MCA was occluded for 1.5 hours as the animal recovered in its cage. At the end of this period, the animals was reanesthetized, and the filament removed to allow for reperfusion; Stroke was induced in $N = 6$ rats, with no mortalities throughout the entire duration of the experiments.

21.1 T Magnetic Resonance Imaging System and Experimental Timeline

All experiments in this study were performed at the NHMFL using the 21.1 T magnet, operating at 900 MHz for protons. The system is equipped with a Bruker Avance III console (Bruker BioSpin, Billerica, MA, USA) and a RRI (Resonance Research, Billerica, MA, USA) gradient system capable of producing up to 600 mT/m in all directions. Excitations and signal acquisitions were performed using a custom-built quadrature dual coil designed for optimal operation on the rat head. Anesthesia was induced using 5% isoflurane in 100% medical grade O_2 and subsequently maintained with 2% isoflurane. Respiratory rates were monitored throughout the experiments, which were performed with respiratory gating. Animals were scanned at 3 hours, 24 hours, and 1 week after ischemia.

^{1}H Longitudinal Relaxation Enhancement Magnetic Resonance Spectroscopy

The localized LRE sequence used in this study is shown in Figure 1. Its main features are spectrally selective excitation and refocusing pulses that avoid the bulk water magnetization,[27] thanks to a band-selective design based on the Shinar–LeRoux algorithm.[31] The 8-ms excitation pulse was modulated to target solely the four methyl resonances of Lac, NAA, Cre, and Cho, with $\leqslant 0.15$ p.p.m. bandwidths for each; this design ensures in turn a minimal perturbation of the pools of aqueous and macromolecular protons that could partake of LRE effects, while avoiding some of the associated J-coupling evolution effects (for instance, from Lactate's methyl coupling partner), which could potentially result in spectral distortions. Under these conditions, the pulse nutation imparted on the water resonance was $< 0.5°$, leaving 99.98% of water protons unperturbed. Because resonances during this relatively long polychromatic excitation pulse were subject to a chemical shift-induced phase evolution, they were refocused subsequently using a pair of frequency-swept adiabatic pulses (each of them 4 ms) that also avoided water perturbations. Spectral selectivity was complemented by a spatial localization imparted by a 3D-LASER module, utilizing three pairs of spatially selective adiabatic frequency-swept refocusing pulses of 5 ms each.[32] To facilitate the quantification of the LRE, a comparison between the spectrally selective sequence was performed against a water-suppressed counterpart, whereby the initial excitation was preceded by a 228-ms Chemical Shift Selective water suppression module[33] (Figure 1).

Magnetic Resonance Imaging Scouts and Voxel Localization

Before the MRS experiments, T_2-weighted images of the rat brain were acquired at all the stroke recovery time points. These MRI scans used a spin-echo Rapid Acquisition with Relaxation Enhancement (RARE) sequence with TR/TE = 5,000/35 ms, RARE factor 8, spatial resolution $230 \times 230 \times 1000$ $(\mu m)^3$, and 12 slices. The stroke-affected region was determined from these images, and a $(4.8\text{-mm})^3$ voxel in the stroke ipsilateral hemisphere was selected. A second, symmetrically placed voxel of the same size was selected in the contralateral hemisphere in a subsequent experiment. The accurate spatial localization of these sharp-edged voxels was confirmed using MRI by concatenating a LASER module identical to that employed in the MRS sequences with a nonselective spin echo imaging sequence. These three-dimensional T_2-weighted images were also used to align the location of the targeted voxels across the different time points of this longitudinal study, and care was taken to ensure the robust placement of these voxels in identical positions throughout the measurements. Under the LASER localization conditions that were used, we estimate the maximum chemical shift-driven displacement between the voxels associated to the different metabolites, to span under 1 mm. Each voxel was selectively shimmed before T_1 measurements using the broadband-excited water signal, whose typical line widths were 25 to 40 Hz.

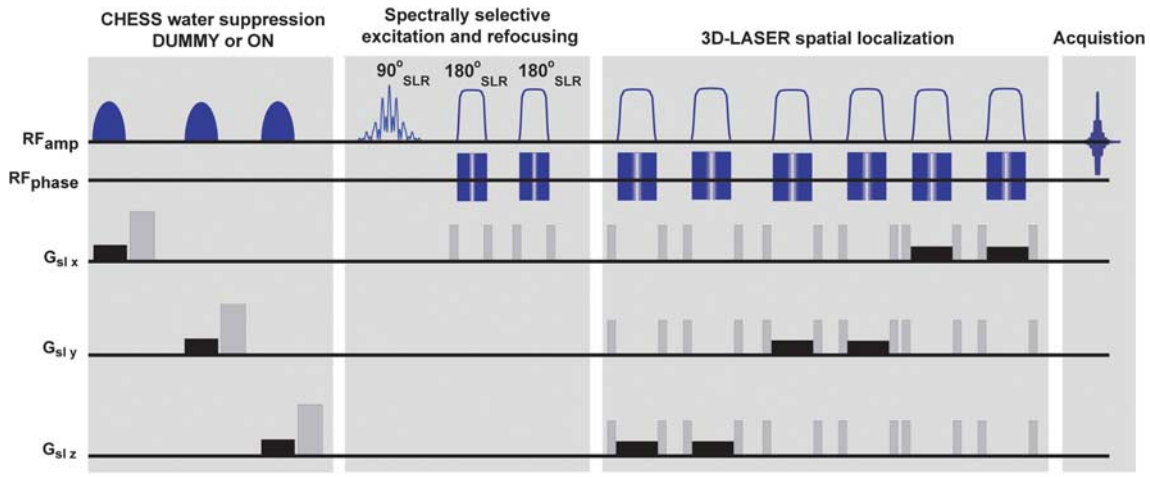

Figure 1. Localized longitudinal relaxation enhancement (LRE) magnetic resonance spectroscopy sequence used to probe apparent metabolic T_1s. The sequence incorporates a spectrally selective module exciting and refocusing only four resonances of interest: lactic acid, *N*-acetylaspartate, creatine, and cholines. The majority of remaining spins in the sample remain unperturbed, thereby facilitating the quantification of LRE effects. Magnetization thus excited is then localized using a 3D-LASER module.[32] To compare water suppressed and non-water suppressed preparations, a chemical shift selective (CHESS) module is played out either in DUMMY mode (i.e., with CHESS pulses off and hence no active form of water suppression), or it is turned ON to observe water-suppressed spectra. A series of eight dummy scans preceded the entire sequence to achieve steady-state magnetization. Crusher gradients are shown in gray, whereas slice-selective gradients are shown in black.

In Vivo T_1 Metabolic Measurements

After ipsi- and contralateral voxels were selected, apparent metabolic T_1s were measured for the rats by a progressive saturation approach[22]. This entailed eight dummy scans and 48 signal averages at a constant echo time of 84 ms, with repetition times incremented from 0.7 to 7.1 s in 15 steps. The order of the repetition times was randomized to avoid any consistency-related bias. For each voxel (ipsi- and contralateral), two sets of apparent T_1 measurements were performed: first, with a LRE sequence leaving all water spins unperturbed (i.e., the chemical shift selective module operated in DUMMY mode), and second, with the LRE sequence preceded by active water excitation and crushing via the chemical shift selective module. Progressive saturation data were fitted to an exponential recovery curve $M(TR) = M_0\left(1 - e^{-\frac{TR}{T_1}}\right) + y_0$, where T_1, M_0 and y_0 (an offset term allowing for non-perfect saturation residue) were the fitted variables. Each T_1-recovery curve took less than 30 minutes to acquire. Out of the 144 T_1s measured (four metabolites x six rats x two methods x three time points), nine were excluded from the analysis owing to the presence of clear acquisition/motion artifacts. To test for statistical differences between groups, an analysis of variance was performed on apparent T_1s with *post hoc* Fisher tests, with $P < 0.05$ considered as the statistically significant threshold. All error bars plotted in this study represent the s.d. across rats.

RESULTS

Figure 2A shows representative T_2-weighted images from a stroke-affected rat 24 hours after ischemia at 21.1 T. Strong hyperintense contrast is evidentproximal to the MCA, clearly delineating the stroke. A representative localization of the ipsi- and contralateral voxels chosen in this study is shown in Figure 2B, overlaid on a dimmed T_2-weighted image of the brain. Notice the sharp spatial localization profiles arising from the LASER module, with magnetization confined to the stroke-affected and healthy regions in the ipsi- and contralateral hemispheres, respectively. Along the third (not explicitly plotted) dimension, these voxels spanned ca. 4.8 mm, corresponding approximately to the slices outlined in a yellow frame in Figure 2A; thus, it was ensured that the ipsilateral voxel contained mostly impaired brain tissue, with minimal partial volume effects from undamaged tissue. The contralateral voxel was symmetrically placed using similar criteria, as shown in Figure 2B. Having achieved the desired spatial specificity, the spectral profiles arising from the addressed voxels was examined via the localized ^{1}H MRS sequence in Figure 1. Representative one-dimensional traces of these spectra are shown in Figure 2B. Features worth highlighting in these data are: the clean, undistorted baselines obtained from the selective echoed excitations; the high spectral specificity reached, with only the four resonances of interest excited (along with another hitherto unassigned peak resonating next to lactate); the nearly complete absence of the water resonance despite the absence of any active form of water suppression; and an excellent signal-to-noise ratios that for NAA in the contralateral hemisphere exceeds 250 in only 48 scans.

Given the high quality of these MRS spectra, robust apparent T_1 measurements in the presence and absence of water suppression were performed. Figure 3 shows characteristic data from progressive saturation experiments, performed *in vivo* on the voxels shown in Figure 2B. In all these experiments, a monotonic magnetization recovery as a function of TR could be clearly observed, with little or no differences in the residual water resonance regardless of whether water suppression was or was not used. The right-hand graphs in Figure 3 show representative examples of fittings performed for data arising from the Cre peak, demonstrating the robustness of these apparent T_1-value quantification. The good quality of these data facilitated repetition of these measurements over a cohort of animals, and for several post-ischemia recovery times. The apparent T_1s obtained in non-water-suppressed and from actively water-suppressed experiments were compared and used to deduce the existence of significant LRE effects in both hemispheres.

Figure 4 summarizes the apparent T_1s obtained for the four metabolites targeted in these studies. These measurements reveal a series of new, metabolite-specific and statistically significant results. First, there is convincing evidence for the presence of LRE effects for Cre at all time points, and for both ipsi- and contralateral voxels. At 3 hours after ischemia and in the ipsilateral hemisphere for instance, the apparent T_1 of Cre increased from 1.5 ± 0.2 to 1.9 ± 0.1 s on performing chemical shift selective water suppression. These effects were statistically significant ($P < 0.0051$, Fisher *post hoc* test), and marked a 27% increase in apparent T_1 on applying active water suppression, which strongly perturbs the

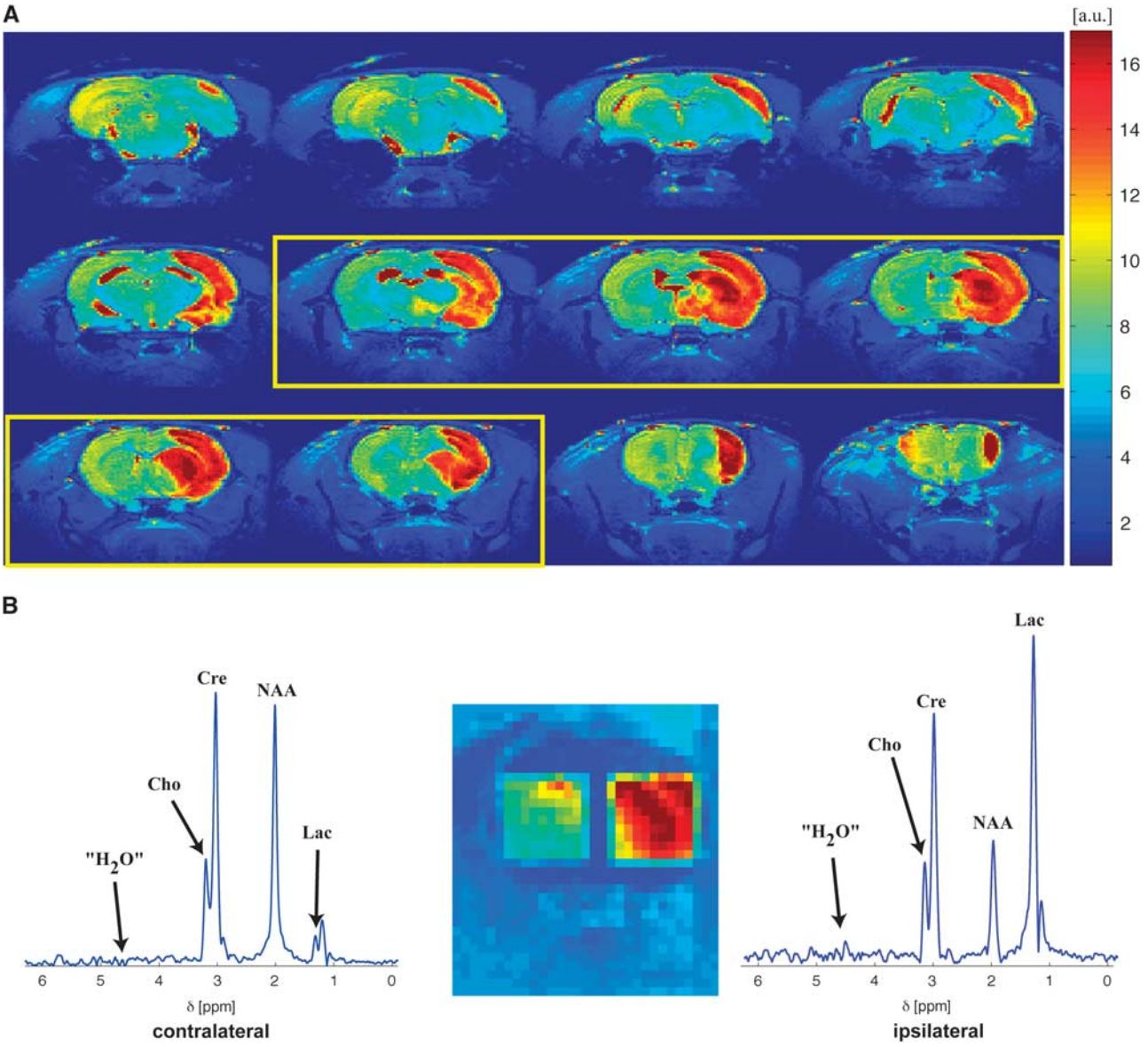

Figure 2. Voxel localization and ensuing ^{1}H magentic resonance spectroscopy (MRS) 21.1 T spectra representative of the data collected in this study. (**A**) T_2-weighted images of the rat brain revealing the strong expected contrast after ischemia between the middle cerebral artery and the territories not affected by stroke. (**B**) The ^{1}H magnetic resonance spectroscopy spectra arising from voxels localized in the ipsi- and contralateral hemispheres, corresponding to the regions indicated in the central image and spanning the yellow outlined slices in (**A**) along the third dimension. Cho, choline; Cre, creatine; Lac, lactic acid; NAA, *N*-acetylaspartate.

water resonance from its M_z equilibrium state. For later time points (24 hours and 1 week after ischemia), ipsilateral Cre LRE was still statistically significant with 16% increases ($P < 0.0048$ and $P < 0.04$, respectively). However, these LREs did not evidence a statistically significant temporal variation between the 3 hours, 24 hours, and 1 week post-ischemia time points. In the contralateral hemisphere, Cre's LRE was also highly consistent and statistically significant ($P < 0.006$) across the different recovery stages, with 21%, 19%, and 21% reductions in the apparent T_1s respectively, on switching from water suppressed to non-water suppressed excitation.

Whereas Cre was the only metabolite showing such consistent LRE effects, a trend was also exhibited by the Lac resonance in the ipsilateral hemisphere: At the 24 hours time point, Lac's apparent T_1 increased from 1.51 ± 0.07 to 1.8 ± 0.3 s on suppressing the water. This LRE was observed in the ipsilateral hemisphere at the 24 hours time point; at 3 hours or 1 week after ischemia LRE effects were not detected, nor were they observed in the contralateral hemisphere. Likewise, the NAA and Cho resonances exhibited no discernible LRE effects at any time point, and their apparent T_1s showed no statistically significant dependencies on their mode of excitation for either of the analyzed voxels.

It is also instructive to follow the temporal evolutions of apparent metabolic T_1s after the ischemia. Figure 5 summarizes these T_1 variations as a function of the post-stroke time elapsed, revealing some common traits but also clear distinctions between the metabolites. The apparent T_1 of Lac responds most dramatically to the onset of ischemia, with a $>50\%$ increase within only 3 hours. By contrast, NAA, Cre, and Cho show no significant modulations at this early time point. At 24 hours, the Lac-apparent

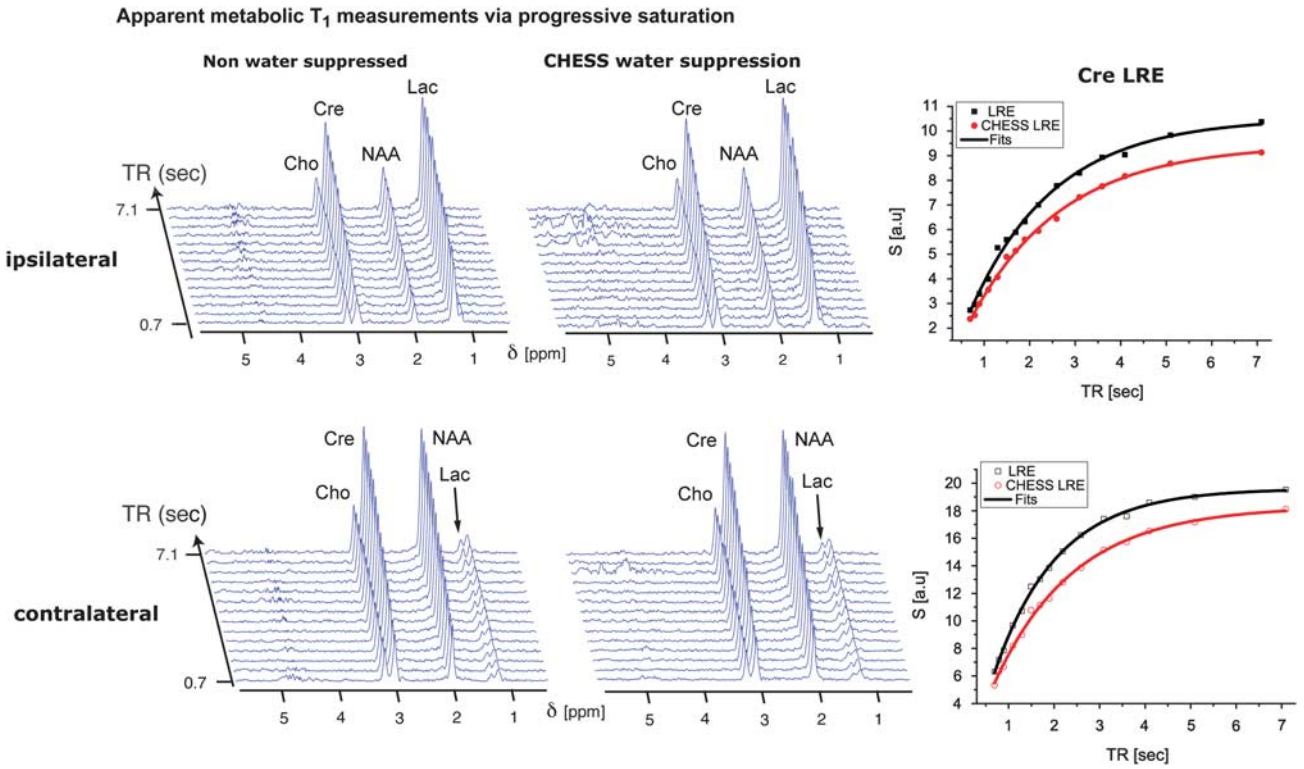

Figure 3. Representative data sets of apparent metabolic T_1 measurements obtained 24hours post ischemia using a progressive saturation (i.e., a variable TR) sequence, arising from the ipsilateral (top panel) and contralateral (bottom panel) hemispheres. Both the non-water-suppressed and water-suppressed one-dimensional traces arose from signal averaging 48 scans over the voxels delineated in Figure 2. Spectra such as these were used for estimating the apparent T_1s in $N = 6$ rats at three different post-ischemic time recovery points. A single T_1-recovery data set took less than 30 minutes to acquire. The right-hand graphs show the fitting of these data for the Cre resonance according to $S(TR) = S_0\left(1 - e^{-\frac{TR}{T_1}}\right) + y_0$, manifesting the LRE effect in both hemispheres. Cho, choline; Cre, creatine; Lac, lactic acid; NAA, *N*-acetylaspartate; TR, repetition time.

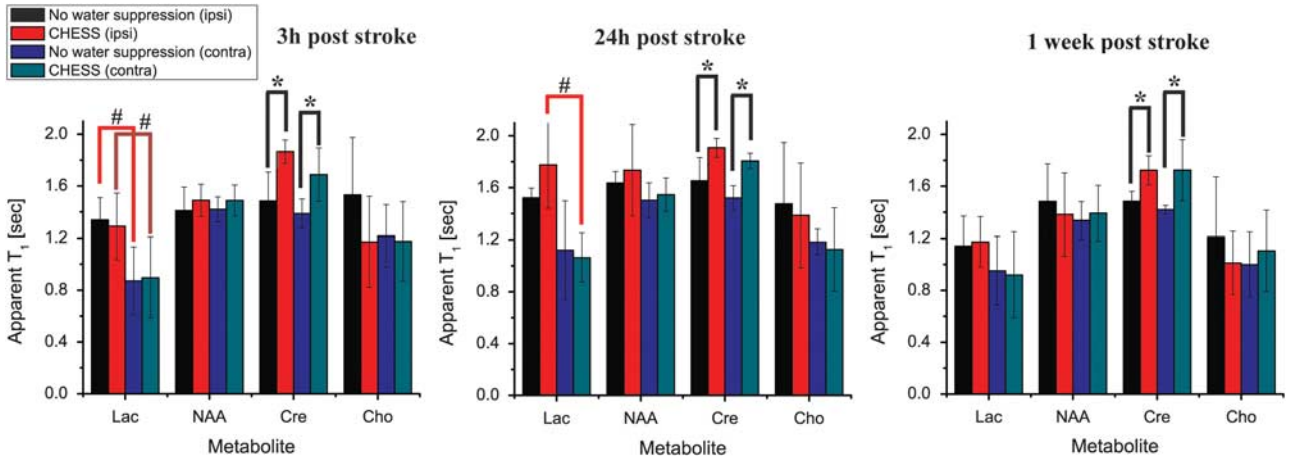

Figure 4. Quantification of the apparent metabolic T_1s extracted from $N = 6$ rats monitored 3 hours, 24 hours, and 1 week after ischemia. Graphs quantify the apparent T_1s observed for voxels in the ipsi- and contralateral hemispheres obtained at each time point, without and with the use of chemical shift selective water suppression. Statistically significant longitudinal relaxation enhancement (LRE) is detected for creatine (Cre) for all time points in both ipsi- and contralateral hemispheres; lactic acid (Lac) shows a LRE trend only 24 hours post ischemia; neither choline (Cho) nor *N*-acetylaspartate (NAA) exhibit definite LRE effects. Symbols represent as follows: $^{*}P < 0.05$ compared with the other method in the same hemisphere; $^{\#}P < 0.05$ compared with the opposite hemisphere with the same method.

T_1 further increases, as do the apparent T_1s of Cre and NAA, which, as mentioned above, were prolonged in a statistically significant fashion. These increases, however, are transient. At the latest time point (1 week after ischemia), NAA, and Cre T_1s returned to baseline levels, exhibiting no statistically significant differences compared with their contralateral counterparts. Interestingly, although reduced compared with the 24-hour post-ischemia time point, Lac's T_1 still has not reverted back to their original baseline

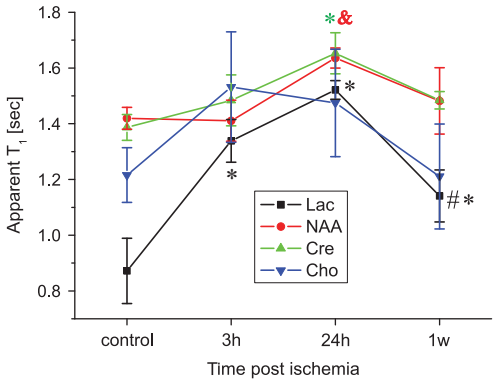

Figure 5. Apparent metabolic T_1 variations at different time points after ischemia revealed by progressive saturation longitudinal relaxation enhancement magnetic resonance spectroscopy. Symbols represent as follows: $^{*}P < 0.05$ compared with contralateral; $^{\&}P < 0.05$ compared with 3 hours; $^{\#}P < 0.05$, compared with 24 hours. Error bars represent the s.e.m.

even at this last time point. Although on average the Cho peak also exhibited a similar dynamic T_1 history, its effects were statistically less reliable (Figure 5).

DISCUSSION

Magnetic resonance spectroscopy can be highly informative, conveying the status of numerous endogenous metabolites within the healthy and diseased tissues.[11,12,34–36] Most MRS measurements report on ratiometric metabolic levels, revealing relative depletions or elevations of certain metabolites as markers of the underlying physiologic processes.[35] Within the context of CNS diseases, the most notable biomarkers are arguably the NAA and Lac peak intensities; depletions in the former are thought to reflect impairments in neuronal viability,[13,35] and elevations in the latter reflect altered bioenergetics and compromised metabolism.[5,14,19] Given a sufficiently good sensitivity, MRS can complement this *in vivo* quantitative insight with more elaborate sources of information: diffusion-weighted MRS, for instance, can potentially convey cellular-specific information on the tissue's microarchitecture and its response to an ischemic insult,[16,37] and relaxation rates[22–24] can inform about the interactions between metabolites and their environment. Despite this potential, relaxation-based MRS experiments have been rather scarce in the context of disease, especially in animal models,[12,18,24] probably owing to the low sensitivity associated to such measurements. A major goal of this study was to exploit the excellent sensitivity that ultrahigh field operation and spectrally selective sequences can endow to ^{1}H MRS, to investigate T_1 relaxation and the potential existence of LRE effects for *in vivo* models of ischemia. In this regard, it should be stressed that LRE provides a different contrast from standard, broadband T_1 measurements, as it measures the changes in apparent T_1 with and without cross-relaxation contributions from other spins.[25,26]

The existence of such LRE effects—that are widely known to influence labile amide but also side chain groups in biomolecular NMR[38]—for the non-labile methyl resonances of metabolites in tissues, can be rationalized by a number of complementary mechanisms. One rests on a process whereby free metabolites exchange with a significant—even if spectrally invisible—population that effectively possesses longer correlation times owing to association with macromolecules; this in turn would affect the relaxation times of the observable metabolic signals differentially, depending on whether these potential cross-relaxation sources are excited or not. Similarly, concurrent macromolecular association of the metabolites and of water molecules could lead to mutual cross-relaxation effects, which do not arise when the metabolites are simply dissolved in solutions. Either of these effects could lead to apparent metabolic relaxation time measurements that depend on whether the spectral excitations are broadband or selective, thereby highlighting the connection between the observed LREs, and the interactions between metabolites and their environment.

A major goal of this study was to investigate whether metabolic LREs could exist *in vivo*. Out of the four metabolic peaks that were targeted, statistically significant *in vivo* LREs were documented for the Cre resonance at 21.1 T; this was apparent in both the ipsi- and contralateral hemispheres of stroke-affected rats, for all recovery times examined after ischemia. These LREs are consistent with previous *in vivo* reports of 'magnetic couplings' between water and the Cre methyl resonance:[28,29] qualitative observations of signal differences in the Cre resonance on water inversion, can now be quantified and explained via an effective modulation of the resonance's apparent T_1. As direct proton exchanges between the Cre methyl group and water is impossible, and as LREs are not observed in aqueous Cre solutions, Cre's *in vivo* LRE mechanism could arise from either an intermolecular $H_2O \rightarrow$ Cre cross-relaxation facilitated as described above; or from rapid exchanges between the water and labile protons in the Cre carbamimidoyl group that are affected by the tissue, and which can impact the methyl proton's relaxation via intramolecular Overhauser effects. A similar source of potential LRE effects could be postulated for the overlapping phosphocreatine peak, but based on additional exchanges between water and the phosphate hydroxyl groups. Further studies of these potential mechanisms are required to discern the exact mechanism leading to LREs *in vivo*.

Despite this clear observation of Cre LRE *in vivo*, our experiments also suggest that these effects are not significantly altered by the onset of ischemia: the magnitudes of Cre's LREs were statistically identical for ipsi- and contralateral hemispheres at 21.1 T, and did not change as a function of recovery time. Therefore, it appears that at 21.1 T Cre LREs are not good candidates as stroke biomarkers. Better potential diagnostic value appears to stem from the Lac resonance, which showed an increased LRE trend 24 h after ischemia for the ipsilateral hemisphere, but exhibited no such effects at other time points or in the contralateral hemisphere. Interestingly, Lac underwent highly statistically significant LRE when brains were subject to the most extreme ischemic conditions at 9.4 T,[27] with LRE measurements performed *ex vivo* at ~3 hours post mortem. Combined, these findings suggest that Lac LREs may become—pending further elucidations of the origins of this phenomenon—an interesting candidate for gaining insights into biochemical processes underlying stroke. Further studies testing larger animal cohorts, stroke outcomes, and different field strengths are required to establish these links.

In agreement with findings presented in a previous 9.4 T *ex vivo* report,[27] NAA does not exhibit any significant LRE *in vivo*—neither in the contralateral nor ipsilateral hemisphere. Interestingly, the NAA resonance's intensity—which correlates with its concentration in the tissue—drops as early as 3 hours after ischemia,[13,35,39] and is generally considered an important biomarker for neuronal viability. The absence of LRE for the NAA methyl resonance may be indicative of either a weak binding to macromolecules (which would be consistent with its negatively charged nature at physiologic pH) or an absence of easily exchangeable protons that would participate in an intramolecular Overhauser relaxation. By contrast with what had been observed in a previous *ex vivo* report[27], Cho also fails to reveal statistically significant LRE *in vivo* at 21.1 T. This could arise from intrinsic differences between *in* and *ex vivo* tissues such as pH; further examinations of this difference are also in progress.

As part of the LRE measurements involved in this study, the *in vivo* evolutions of metabolic T_1s for the targeted methyl peaks were also followed at 21.1 T. A number of features are worth highlighting from this longitudinal post-ischemia study. First, it appears that metabolic T_1s for the targeted resonances do not increase with increasing fields. Indeed, a previous study comparing metabolic T_1s in normal *in vivo* rat brains at 4, 9.4, and 11.7 T suggested an increase in T_1s up to 7 T and a leveling off thereafter;[23] subsequent studies extended these findings to 14.1 T.[22] The present work finds that the metabolic relaxation times for the contralateral NAA, Cre and to a certain extent Cho peaks at 21.1 T, closely resemble those found previously at 9.4, 11.7 and 14.1 T in normal animals. This finding is suggestive of intricate interactions between the metabolites and their host tissue, as this behavior significantly departs from the one exhibited, for example, by the water resonance. Another feature that emerges from these metabolic T_1 measurements is a clear longitudinal evolution after ischemia. Whereas NAA, Cre, and Cho T_1s are known to increase only 24h after ischemia[18,21] (findings that were herein also confirmed at 21.1 T), we find much more rapid dynamics for the Lac resonance. Lac's apparent T_1 increases by more than 50% from its baseline value as early as 3 hours after ischemia; interestingly, this timescale parallels the onset of cytotoxic edema arising from anaerobic glycolysis and the ensuing ischemic cascade[3]. It follows that Lac T_1s are highly sensitive probes of the tissue's response to ischemia, especially in comparison with the slow T_1 dynamics exhibited by the other metabolic signals, which are more indicative of the onset of vasogenic edema at the 24-h time point[18]. Although the mechanisms of these fast Lac T_1 dynamics remain to be elucidated, the absence of similar LRE effects in free solutions suggests a role for this metabolite's binding to tissue macromolecules. Understanding such T_1 changes and potential LRE effects for these upfield resonances[27]—as well as for downfield peaks[27,40]—may help in understanding the processes underlying ischemia from the point of insult to recovery, as well as in studying novel biomarkers for the ischemic penumbra and functional outcomes of stroke.

CONCLUSIONS

This paper examined, for the first time, *in vivo* evidence for metabolic LRE effects and changes in the apparent metabolic T_1s in stroke-affected rats at 21.1 T. Differential LRE effects were observed for specific metabolites on switching from water-suppressed acquisitions to non-water-suppressed excitation modes, shedding light on the complex interactions of metabolites within ischemic and non-ischemic tissues. Cre's *in vivo* LRE appeared to be stroke independent; by contrast Lac's LRE exhibited an ischemia-dependent evolution. Furthermore, the apparent T_1 of Lac exhibited rapid changes, suggesting this metabolite's sensitivity to the environment created by cytotoxic edema. These aspects of Cre's and Lac's T_1 and LRE effects deserve further systematic studies under normal and diseased conditions to better understand the molecular details associated with stroke and recovery. From a methodological standpoint, it is also worth stressing the remarkably clean and undistorted baselines and the excellent sensitivity that characterized the selectively excited ^{1}H MR spectra shown. These positive characteristics are the result of multiple, mutually reinforcing effects derived from executing this kind of experiment at very high fields, including favorable relaxation properties (which enhance metabolic and suppress water signals), and of course the inherent high sensitivity endowed by recordings at ultrahigh fields. These factors enable rapid multiscan experiments leading to good spatiotemporal resolution, no water signal contamination, excellent signal-to-noise ratios per unit time, as well as very clean baselines. Numerous avenues in the research and diagnosis of the CNS can thus open by this synergy.

DISCLOSURE/CONFLICT OF INTEREST

The authors declare no conflict of interest.

REFERENCES

1 Schaller B, Graf R. Cerebral ischemia and reperfusion: the pathophysiologic concept as a basis for clinical therapy. *J Cereb Blood Flow Metab* 2004; **4**: 351–371.
2 Moskowitz MA, Lo EH, Iadecola C. The science of stroke: mechanisms in search of treatments. *Neuron* 2010; **2**: 181–198.
3 Dreier JP. The role of spreading depression, spreading depolarization and spreading ischemia in neurological disease. *Nat Med* 2011; **4**: 439–447.
4 Dijkhuizen RM, Nicolay K. Magnetic resonance imaging in experimental models of brain disorders. *J Cereb Blood Flow Metab* 2003; **12**: 1383–1402.
5 Weber R, Ramos-Cabrer P, Hoehn M. Present status of magnetic resonance imaging and spectroscopy in animal stroke models. *J Cereb Blood Flow Metab* 2006; **5**: 591–604.
6 Baird AE, Warach S. Magnetic resonance imaging of acute stroke. *J Cereb Blood Flow Metab* 1998; **6**: 583–609.
7 Moseley ME, Decrespigny AJS, Roberts TPL, Kozniewska E, Kucharczyk J. Early detection of regional cerebral-ischemia using high-speed MRI. *Stroke* 1993; **12**: I60–I65.
8 Kakuda W, Lansberg MG, Thijs VN, Kemp SM, Bammer R, Wechsler LR *et al*. Optimal definition for PWI/DWI mismatch in acute ischemic stroke patients. *J Cereb Blood Flow Metab* 2008; **5**: 887–891.
9 Weber R, Ramos-Cabrer P, Justicia C, Wiedermann D, Strecker C, Sprenger C *et al*. Early prediction of functional recovery after experimental stroke: functional magnetic resonance imaging, electrophysiology, and behavioral testing in rats. *J Neurosci* 2008; **5**: 1022–1029.
10 Dijkhuizen RM, Ren JM, Mandeville JB, Wu ON, Ozdag FM, Moskowitz MA *et al*. Functional magnetic resonance imaging of reorganization in rat brain after stroke. *Proc Nat Acad Sci USA* 2001; **22**: 12766–12771.
11 de Graaf RA. *In-Vivo NMR Spectroscopy: Principles and Techniques*. 2nd edn. John Wiley and Sons Ltd.: Chichester, England, 2007.
12 Duarte JMN, Lei HX, Mlynarik V, Gruetter R. The neurochemical profile quantified by *in vivo* H-1 NMR spectroscopy. *Neuroimage* 2012; **2**: 342–362.
13 Demougeot C, Garnier P, Mossiat C, Bertrand N, Giroud M, Beley A *et al*. N-Acetylaspartate, a marker of both cellular dysfunction and neuronal loss: its relevance to studies of acute brain injury. *J Neurochem* 2001; **2**: 408–415.
14 Coon AL, Arias-Mendoza F, Colby GP, Cruz-Lobo J, Mocco J, Mack WJ *et al*. Correlation of cerebral metabolites with functional outcome in experimental primate stroke using in vivo H-1-magnetic resonance spectroscopy. *Am J Neuroradiol* 2006; **5**: 1053–1058.
15 Parsons MW, Li T, Barber PA, Yang Q, Darby DG, Desmond PM *et al*. Combined H-1 MR spectroscopy and diffusion-weighted MRI improves the prediction of stroke outcome. *Neurology* 2000; **4**: 498–505.
16 Dijkhuizen RM, de Graaf RA, Tulleken KAF, Nicolay K. Changes in the diffusion of water and intracellular metabolites after excitotoxic injury and global ischemia in neonatal rat brain. *J Cereb Blood Flow Metab* 1999; **3**: 341–349.
17 Dreher W, Busch E, Leibfritz D. Changes in apparent diffusion coefficients of metabolites in rat brain after middle cerebral artery occlusion measured by proton magnetic resonance spectroscopy. *Magn Reson Med* 2001; **3**: 383–389.
18 van der Toorn A, Dijkhuizen RM, Tulleken CAF, Nicolay K. T-1 and T-2 relaxation times of the major H-1-containing metabolites in rat brain after focal ischemia. *NMR Biomed* 1995; **6**: 245–252.
19 Cady EB. Metabolite concentrations and relaxation in perinatal cerebral hypoxic-ischemic injury. *Neurochem Res* 1996; **9**: 1043–1052.
20 Fujimori H, Michaelis T, Wick M, Frahm J. Proton T-2 relaxation of cerebral metabolites during transient global ischemia in rat brain. *Magn Reson Med* 1998; **4**: 647–650.
21 Cheong JLY, Cady EB, Penrice J, Wyatt JS, Cox IJ, Robertson NJ. Proton MR spectroscopy in neonates with perinatal cerebral hypoxic-ischemic injury: Metabolite peak-area ratios, relaxation times, and absolute concentrations. *Am J Neuroradiol* 2006; **7**: 1546–1554.
22 Cudalbu C, Mlynarik V, Xin LJ, Gruetter R. Comparison of T-1 relaxation times of the neurochemical profile in rat brain at 9.4 Tesla and 14.1 Tesla. *Magn Reson Med* 2009; **4**: 862–867.
23 de Graaf RA, Brown PB, McIntyre S, Nixon TW, Behar KL, Rothman DL. High magnetic field water and metabolite proton T-1 and T-2 relaxation in rat brain *in vivo*. *Magn Reson Med* 2006; **2**: 386–394.
24 Lei H, Zhang Y, Zhu XH, Chen W. Changes in the proton T-2 relaxation times of cerebral water and metabolites during forebrain ischemia in rat at 9.4 T. *Magn Reson Med* 2003; **6**: 979–984.
25 Pervushin K, Vogeli B, Eletsky A. Longitudinal H-1 relaxation optimization in TROSY NMR spectroscopy. *J Am Chem Soc* 2002; **43**: 12898–12902.

26 Schanda P. Fast-pulsing longitudinal relaxation optimized techniques: enriching the toolbox of fast biomolecular NMR spectroscopy. *Prog Nucl Magn Reson Spectrosc* 2009; **3**: 238–265.
27 Shemesh N, Dumez JN, Frydman L. Longitudinal relaxation enhancement in H-1 NMR spectroscopy of tissue metabolites via spectrally selective excitation. *Chemistry* 2013; **39**: 13002–13008.
28 Kruiskamp MJ, de Graaf RA, van Vliet G, Nicolay K. Magnetic coupling of creatine/phosphocreatine protons in rat skeletal muscle, as studied by H-1-magnetization transfer MRS. *Magn Reson Med* 1999; **4**: 665–672.
29 Leibfritz D, Dreher W. Magnetization transfer MRS. *NMR Biomed* 2001; **2**: 65–76.
30 Luo Y, Rydzewski J, de Graaf RA, Gruetter R, Garwood M, Schleich T. *In vivo* observation of lactate methyl proton magnetization transfer in rat C6 glioma. *Magn Reson Med* 1999; **41**: 676–685.
31 Pauly J, Leroux P, Nishimura D, Macovski A. Parameter relations for the Shinnar-Leroux selective excitation pulse design algorithm. *IEEE Trans Med Imaging* 1991; **1**: 53–65.
32 Garwood M, DelaBarre L. The return of the frequency sweep: designing adiabatic pulses for contemporary NMR. *J Magn Reson* 2001; **2**: 155–177.
33 Haase A, Frahm J, Hanicke W, Matthaei D. H-1-NMR chemical-shift selective (Chess) imaging. *Phys Med Biol* 1985; **4**: 341–344.
34 Govindaraju V, Young K, Maudsley AA. Proton NMR chemical shifts and coupling constants for brain metabolites. *NMR Biomed* 2000; **3**: 129–153.
35 Demougeot C, Bertrand N, Prigent-Tessier A, Garnier P, Mossiat C, Giroud M *et al.* Reversible loss of N-acetyl-aspartate in rats subjected to long-term focal cerebral ischemia. *J Cereb Blood Flow Metab* 2003; **4**: 482–489.
36 Franke C, Brinker G, Pillekamp F, Hoehn M. Probability of metabolic tissue recovery after thrombolytic treatment of experimental stroke: A magnetic resonance spectroscopic imaging study in rat brain. *J Cereb Blood Flow Metab* 2000; **3**: 583–591.
37 Nicolay K, Braun KPJ, de Graaf RA, Dijkhuizen RM, Kruiskamp MJ. Diffusion NMR spectroscopy. *NMR Biomed* 2001; **2**: 94–111.
38 Schanda P, Brutscher B. Very fast two-dimensional NMR spectroscopy for real-time investigation of dynamic events in proteins on the time scale of seconds. *J Am Chem Soc* 2005; **22**: 8014–8015.
39 Sager TN, Laursen H, Fink-Jensen A, Topp S, Stensgaard A, Hedehus M *et al.* N-acetylaspartate distribution in rat brain striatum during acute brain ischemia. *J Cereb Blood Flow Metab* 1999; **2**: 164–172.
40 de Graaf RA, Behar KL. Detection of cerebral NAD+ by 1H NMR spectroscopy. *NMR Biomed* 2014; **27**: 802–809.